Journal of Applied Polymer Science

Preparation and characterization of Silicalite-1/PDMS surface sieving pervaporation membrane for separation of ethanol/water mixture

Xiangyan Liu,[1,2] Deng Hu,[1] Meng Li,[1] Jianming Zhang,[1] Zhigao Zhu,[1] Gaofeng Zeng,[1] Yanfeng Zhang,[1,3] Yuhan Sun[1,3]

[1]CAS Key Laboratory of Low-carbon Conversion Science and Engineering, Shanghai Advanced Research Institute, Chinese Academy of Sciences, 100 Haike Rd, Shanghai, 201210, China

[2]University of Chinese Academy of Sciences, 19 Yuquan Rd, Shijingshan District, Beijing, 100049, China

[3]School of Physical Science and Technology, ShanghaiTech University, Shanghai 201210, China

Correspondence to: Yanfeng Zhang (E-mail: zhangyf@sari.ac.cn)

ABSTRACT: To improve the pervaporation performance of Silicalite-1/PDMS composite membrane by adding a small amount of Silicalite-1 zeolite, novel Silicalite-1/PDMS surface sieving membranes (SSMs) were prepared by attaching Silicalite-1 particles on the PDMS membrane surface. The obtained membranes and traditional mixed-matrix membranes (MMMs) were characterized by SEM, XRD, TGA, FT-IR, and pervaporation separation of ethanol–water mixture. Effects of Silicalite-1 particles content, feed temperatures, and feed compositions on the separation performance were discussed. From the cross-section view SEM images of SSMs, a two-layer structure was observed. The thickness of the Silicalite-1 layer was about 300 nm to 2 μm. The TGA analysis indicates that the zeolite concentration in 3 wt % SSM is lower than 10 wt % MMMs. In the ethanol/water pervaporation experiment, the separation factor of Silicalite-1/PDMS SSMs increased considerably compared with pure PDMS membrane. When the suspensions concentrations of Silicalite-1 particles reached 3 wt %, the separation factor was about 217% increase over pure PDMS membrane and 52.9% increase over 10 wt % Silicalite-1/PDMS MMMs. As the ethanol concentration in the feed increases, the separation factor of SSMs increases, whereas permeation flux decreases. At the same time, with increasing operating temperature, the permeation flux of SSMs increased. The stability of SSMs at high temperature is better than the traditional MMMs. © 2015 Wiley Periodicals, Inc. J. Appl. Polym. Sci. **2015**, *132*, 42460.

KEYWORDS: membranes; nanoparticles; nanowires and nanocrystals; properties and characterization; separation techniques

Received 28 January 2015; accepted 4 May 2015

DOI: 10.1002/app.42460

INTRODUCTION

Pervaporation is a membrane process to separate liquid mixtures. A heated liquid mixture is fed to the membrane surface and the permeate vapor is removed from the back of the membrane and collected under low temperature. Unlike distillation process, which takes advantage of the relative volatility of the feed components, the pervaporation is based on the difference in sorption and diffusion properties of the feed components and permselectivity of the membrane.[1–3] Compared with traditional distillation technology, pervaporation is energy efficient. During pervaporation, only the permeate was vaporized, which leads to substantial energy saving. The process has already been applied to solvent dehydration, separation of dissolved organics from water, and separation of organic mixtures.[4–9]

Hydrophobic silicone rubber is considered as a potential material for the separation of volatile organic compounds (VOCs) from water. Polydimethylsiloxane (PDMS) has already been used for pervaporation of organics/inorganics mixture.[10–17] Jadav *et al.*[10] prepared high flux PDMS membranes for separation of organics from water by pervaporation. The influence of film thickness on the structure and properties of PDMS membrane was studied. Thinner membrane had a relatively loose structure, which resulted into low selectivity and high flux. Zhan *et al.*[11] prepared multilayer PDMS/PVDF composite membranes with an alternative PDMS/PVDF/nonwoven–fiber/PVDF/PDMS configuration. The composite membrane gave separation factor of 15 and permeation rate of 0.45 $kg.m^{-2}.h^{-1}$ for 5 wt % ethanol feed at 60°C. Liu *et al.*[18] developed c-PDMS/BPPO composite membrane supported by ceramic tube for pervaporation separation of butanol from water. When the bromide-substituted ratio was 34 wt %, the composite membrane exhibited a separation factor of 35 and a flux of 0.22 $kg.m^{-2}.h^{-1}$ for 5 wt % butanol–water mixture at 40°C, and the downstream

pressure was 0.1 kPa. Niemistö *et al.*[19] studied the performance of PDMS membrane with a support layer of polyacrylonitrile (PAN) for the removal of acetone, butanol, and ethanol from dilute aqueous model solutions. Results indicated that the tested membrane has potential to be used in the acetone–butanol–ethanol fermentation process.

In addition to polymer membranes, there has been an increasing interest in mixed matrix membrane. Mixed-matrix membranes (MMMs), first reported by UOP,[20,21] may surpass the trade-off limit of permeability verse selectivity, by combining the easy processability and low cost of polymer materials with the excellent separation properties of inorganic molecular sieves. Nanoporous molecular sieving materials (like carbon molecular sieves, zeolites, metal-organic frameworks) are common additives for mixed-matrix membranes.[22–24] At choice of nanoporous molecular sieving materials, studies have been focused of choosing different nanomaterials or zeolite with special feature to prepare the PDMS MMMs to enhance the performance of the membranes.[25–27] Hydrophobic Silicalite-1 zeolite was added into polymer membranes for pervaporation separation of ethanol–water mixture.[28–33] Yi *et al.*[29] improved the affinity between Silicalite-1 and PDMS by modifying the Silicalite-1 particles with vinyltriethoxysilane (VTES). The thermal stability of Silicalite-1/PDMS hybrid membrane has been improved. Compared with the unmodified MMMs, the VTES modified Silicalite-1/PDMS MMMs effectively improved the pervaporation selectivity at different Silicalite-1 loading. Despite tremendous research effort, the traditional MMMs still have many issues to be solved, like poor interfacial contact, marginal improvement in performance, and poor mechanical properties. To realize reasonable performance increase, the zeolite loading usually need to be at least 30 wt %, which leads to poor mechanical stability. Recently, Zheng *et al.*[34] proposed a novel surface sieving membrane by attaching zeolite crystals onto polymer membrane surface. The obtained hybrid membranes exhibited 300% increase in separation factor for methanol–dimethyl carbonate separation without sacrificing mechanical properties.

The goal of this work was to investigate the possibility of obtaining novel membranes, surface sieving membranes (SSMs), with high permeation flux and selectivity. In this work, PDMS and Silicalite-1 zeolite were used to prepare PDMS pure membrane, Silicalite-1/PDMS MMMs and Silicalite-1/PDMS SSMs. The membranes performances in terms of permeation flux and ethanol–water separation factor were evaluated by a custom-made pervaporation system and the membranes structures and chemical alterations were characterized by scanning electron microscope (SEM), X-ray diffraction (XRD), thermogravimetric analysis (TGA), and Fourier-transform infrared spectroscopy (FT-IR). Different pervaporation and test conditions on membranes performance were investigated.

EXPERIMENTAL

Materials

Polydimethylsiloxane (PDMS) (Liquid silicone rubber C6-530, part A & B) was purchased from Dow Corning Corporation, China. Tetraethyl orthosilicate (TEOS) was obtained from Aladdin Chemistry Co. Tetrapropylammonium hydroxide (TPAOH, 25 wt %) was supplied by Shanghai Nuotai Chemical Co. Anhydrous ethanol and *n*-hexane were purchased from Shanghai Richjoint Chemical Reagents Co. All the chemicals were used without further purification.

Zeolite Preparation

The Silicalite-1 zeolite crystals were prepared by a two-step microwave-assisted hydrothermal synthesis according to the literature.[35] The gel molar ratio was $1.0SiO_2$: 0.4TPAOH : $19.5H_2O$: $4.0C_2H_5OH$. The mixture was stirred for 24 h at 25°C and transferred into a Teflon-lined stainless steel autoclave for the microwave-assisted hydrothermal treatment. The synthesis parameters were as follows: 80°C for 90 min and at 180°C for 60 min. After cooling down the autoclave, the Silicalite-1 zeolite crystals were centrifuged and washed thoroughly. The obtained zeolite product was calcined at 600°C for 8 h in air for template removal.

Membrane Preparation

Preparation of Pure PDMS Membrane. The pure PDMS membrane was prepared by solution casting method. The casting solution was prepared by dissolving liquid silicone rubber C6–530 part A and part B (1 : 1 ratio) in a given amount of *n*-heptane under stirring at room temperature for about 4 h. After degassing under vacuum, membrane was cast onto a nonporous polytetrafluoroethylene (PTFE) substrate using a stainless steel knife. The solution was heated at 50°C for 5 h to remove the solvent and then cured in a vacuum oven at 80°C for another 5 h. After peeling off the membrane from the PTFE substrate, a free-standing PDMS membrane was obtained.

Preparation of Silicalite-1/PDMS Mixed Matrix Membranes. The calcined Silicalite-1 particles were dried at 200°C for 24 h in a vacuum oven. First, a desired amount of Silicalite-1 particles were mixed with a given amount of *n*-heptane under ultrasonic dispersion at room temperature for 0.5 h. Then, a small amount of diluted PDMS solution (5 wt %) was added and stirred for 1 h until the Silicalite-1 particles were coated by PDMS. Last, the rest of PDMS solution (50 wt %) was added (to reach desired Silicalite-1/PDMS ratio) and stirred for 3 h. The rest operation steps were the same as the preparation of pure PDMS membrane. After peeling off the membrane from the PTFE substrate, Silicalite-1/PDMS MMMs were obtained.

Preparation of Silicalite-1/PDMS Surface Sieving Membranes. The calcined Silicalite-1 particles were dispersed in anhydrous ethanol to make 0.4–3.0 wt % suspensions. Extensive sonication was used to disperse the Silicalite-1 particles. Silicalite-1 particles were deposited onto a nonporous PTFE substrate by dip coating method. The clean PTFE film was soaked in the zeolite suspension for 30 s, and then withdrew by a dip coater at a 200 μm/s rate. The dip-coated PTFE was dried at room temperature for 1 h. Then, PDMS membrane was cast on the PTFE substrate pre-coated with Silicalite-1 crystals. After peeling off the membrane from the PTFE substrate, Silicalite-1/PDMS SSMs were obtained.

Characterization

The surface and cross-section of MMMs and SSMs were examined by a scanning electron microscope (Hitachi S4800). The

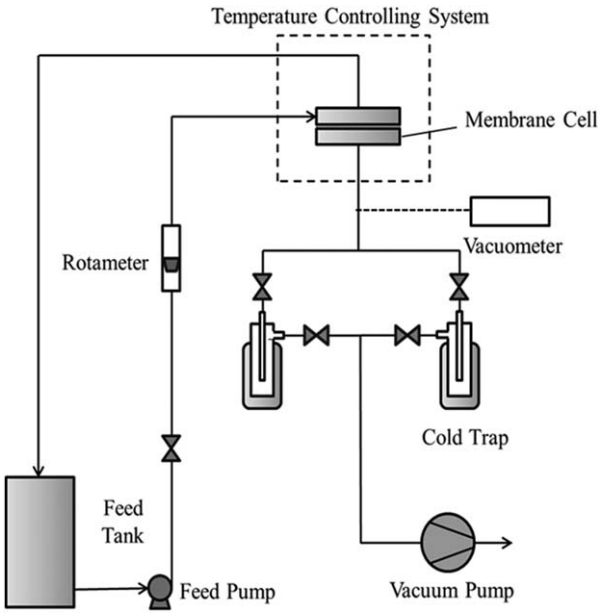

Figure 1. Schematic diagram of pervaporation apparatus.

membrane cross-section samples were prepared by freeze-fracture method. All the samples were coated with gold before observation.

X-ray diffraction (XRD) patterns of the Silicalite-1 particles, MMMs, and SSMs were obtained with a Rigaku Ultima IV X-ray diffractometer (tube voltage: 40 kV and tube current: 40 mA).

Thermal degradation measurements of the MMMs and SSMs were performed using a thermogravimetric analyzer (TGA) (NETZSCH, STA 449F3). All samples were tested from room temperature to 1000°C with a heating rate of 10°C/min in a nitrogen flow of 50 mL/min.

Infrared spectra were collected with a Fourier-transform infrared spectrometer (Thermo Scientific, Nicolet 6700).

Pervaporation Measurements

The separation performance of the MMMs and SSMs were obtained by a custom-made pervaporation system, as shown in Figure 1. All experiments were performed for at least three times. All the membranes were 40 mm in diameter. During the experiments, the feed side pressure was maintained at atmospheric pressure and the downstream pressure was kept below 200 Pa all the time. The ethanol concentration in the binary feed solution was 5 wt % and the feed temperature was kept at 50°C.

Before collecting sample, the system was allowed to equilibrate for 3 h to reach a steady state. The permeate sample was collected in a liquid nitrogen cold trap for 3–6 h (depending on the membrane flux). The weight of the collected samples were weighed by a balance and the ethanol concentrations of the feed solution and the permeate were analyzed by a gas chromatograph (GC).

The fluxes were normalized to a membrane thickness of 100 μm assuming an inverse proportionality between the total flux and the membrane thickness. The total flux is defined as follows:

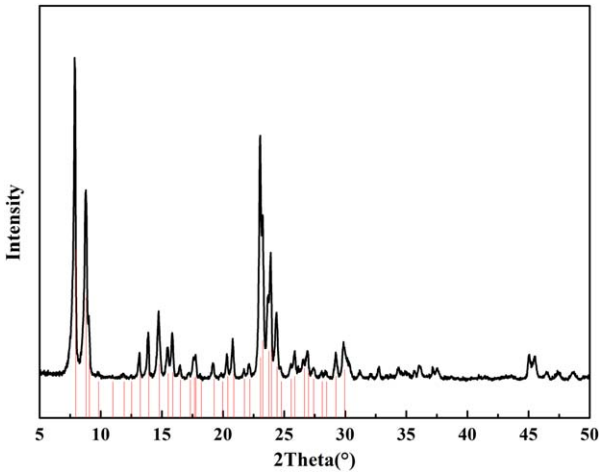

Figure 2. XRD patterns of Silicalite-1 (vertical line: standard pattern from IZA website). [Color figure can be viewed in the online issue, which is available at wileyonlinelibrary.com.]

$$Flux' = (L/100) \cdot Flux = (L/100) \cdot W/(A \cdot t) \quad (1)$$

Where W is the weight of the permeate samples collected during the experiment, A is the effective membrane area (12.6 cm^2 for all membranes), t is the permeation time for sample collection, and L is the membrane thickness. Moreover, the total membrane thickness was about 85 ± 10 μm, as determined by SEM.

The separation factor (α) in this work was calculated using the following equation:

$$\alpha = \frac{Y_{EtOH}/Y_{H_2O}}{X_{EtOH}/X_{H_2O}} \quad (2)$$

Where Y and X are the weight ratio of ethanol and water in the permeate and the feed, respectively.

RESULTS AND DISCUSSION

Characterization of Silicalite-1 Particles

Figure 2 shows the X-ray diffraction pattern of Silicalite-1 particles. It can be seen from Figure 2 that the first two intense peaks at about $2\theta = 7.94°$ and 8.90° corresponding to [0 1 1] and [2 0 0] planes, and another intense diffraction peak at $2\theta = 23.12°$ corresponding to [0 5 1] planes, which were the

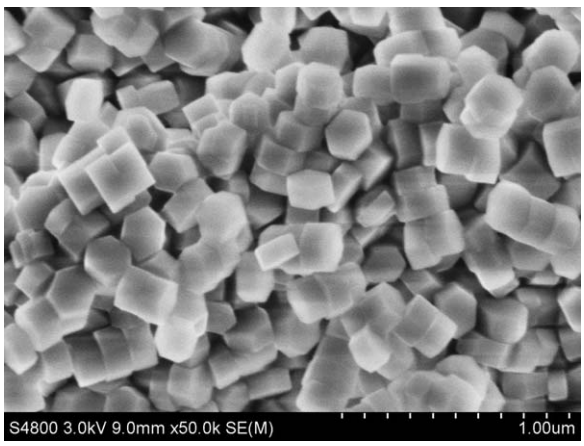

Figure 3. SEM images of Silicalite-1 particles.

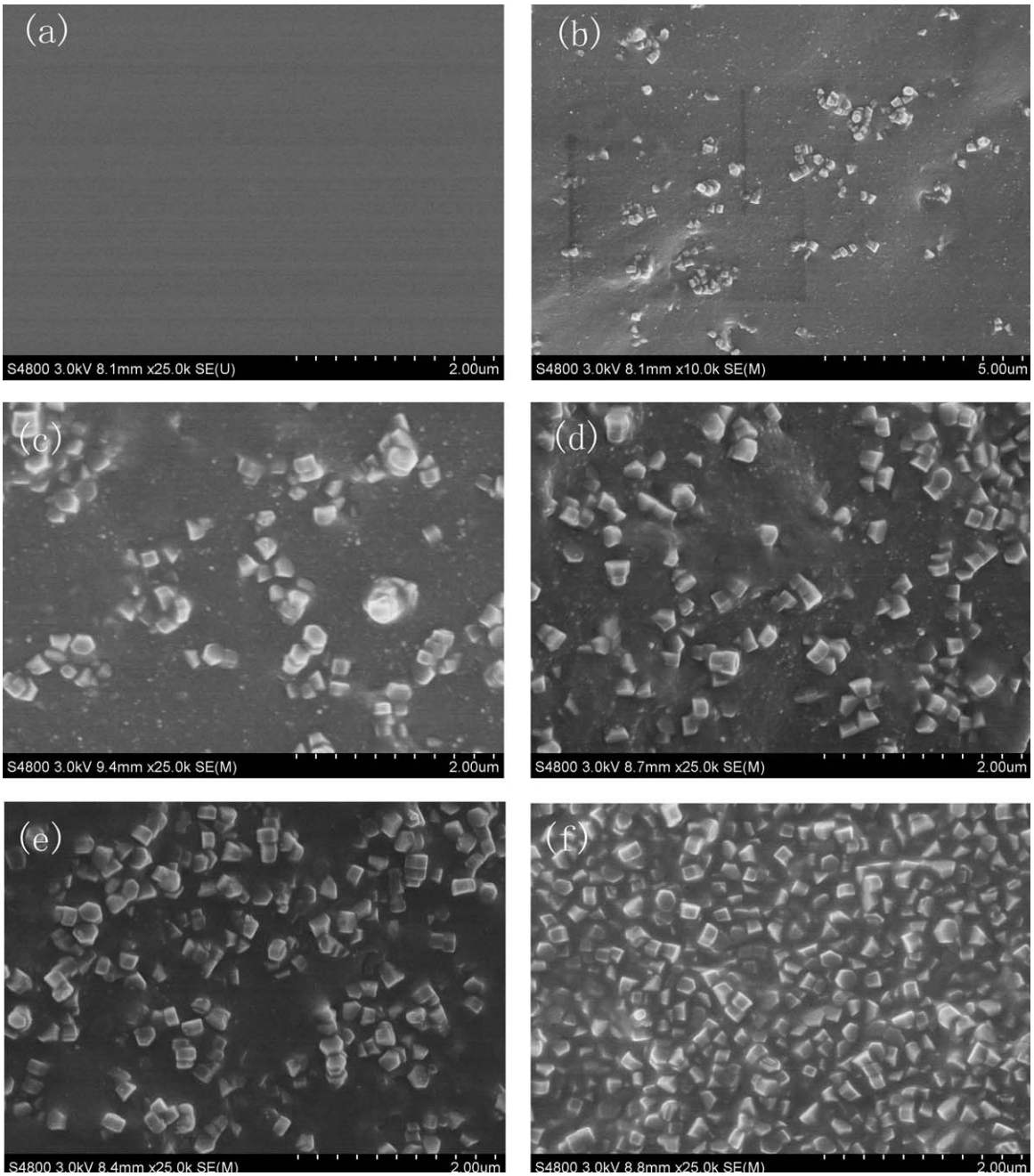

Figure 4. Cross-section view SEM images of PDMS and Silicalite-1/PDMS membranes with different Silicalite-1 loading, (a) 0 wt %, (b) 5 wt %, (c) 10 wt %, (d) 20 wt %, (e) 30wt %, and (f) 40 wt %.

characteristic peaks of MFI type structure.[29] Figure 3 shows the SEM image of Silicalite-1 particles used in this study. As shown in Figure 3, the Silicalite-1 crystals exhibited hexagonal prism morphology, which is typical for MFI zeolite. The crystals have uniform size distribution with diameter ~200 nm and height of 100 nm.

Characterization of Membranes

SEM was used to characterize the distribution of zeolite particles in the MMMs and SSMs. Figure 4 shows the cross-section morphologies of MMMs with different Silicalite-1 particles loadings. The pure PDMS membrane exhibited clean and smooth cross-section, as shown in Figure 4(a), which is typical for pure polymer membrane. From the cross-sectional SEM image of the MMMs, the Silicalite-1 particles were dispersed uniformly in the PDMS matrix and no particles aggregation was observed. As shown in the close-up SEM image [Figure 4(f)], no visible voids were observed at the polymer–zeolite interface. This indicated that good interfacial contact was realized, which is important for MMM. The presence of interfacial voids may lead to the hydrophobic polymer chains from PDMS have good compatibility with hydrophobic Silicalite-1 crystals and the

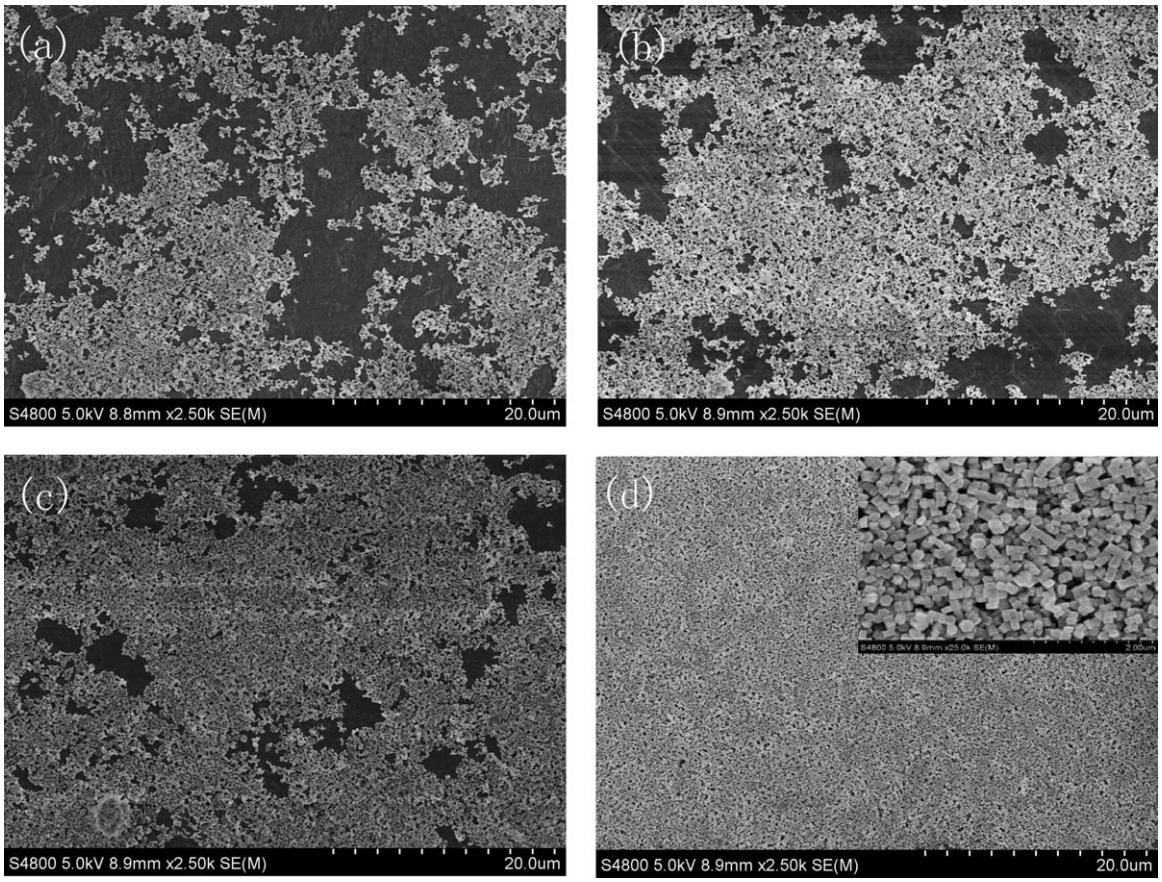

Figure 5. Top view SEM images of PTFE substrates dip-coated in Silicalite-1 particles suspensions with different concentrations, (a) 0.4 wt %, (b) 1.0 wt %, (c) 2.0 wt %, and (d) 3.0 wt %.

flexible polymer chain packing of rubbery PDMS also contributes. With the increase of Silicalite-1 particles loading, more Silicalite-1 particles can be observed from the cross-section images. Even at 40% loading, no Silicalite-1 particles aggregation was observed, which indicated good dispersion. The similar phenomenon was observed by other scholars.[26,36–39]

Figure 5 shows the top view SEM images of PTFE substrates dip-coated in Silicalite-1 particles suspensions with different concentrations. From the top view SEM images of PTFE substrates, the rectangular Silicalite-1 particles can be seen on the substrate surface and the particles coverage increases as concentration of Silicalite-1 particles suspensions increases. When the concentration of Silicalite-1 dip-coating suspension reached 3 wt %, full coverage is obtained. From Figure 5(d), it can be seen that there are more than one layer of crystals on the substrate. However, the thickness of zeolite layer was not checked by SEM, because the SEM sample preparation is difficult. As shown in the close-up SEM image in Figure 5(d), these Silicalite-1 crystals were randomly orientated and the crystals packing were not tight. We hope we can get the single layer and closely arranged crystals as described in the literature in the follow-up studies.[40–42]

Figure 6 shows the cross-sectional SEM images of SSMs prepared with different concentrations of Silicalite-1 particles suspensions. Apparently, a two-layer structure was observed, one layer of clean polymer and one layer of mixed matrix membrane. In the mixed matrix membrane layer, multiple layers of Silicalite-1 particles were observed. The thickness of the Silicalite-1 layer increased from ~300 nm to 2 μm as the zeolite concentration in the dip-coating suspensions increased from 0.4 to 3 wt %. The adhesion between the polymer phase and Silicalite-1 particles was good because no voids and cracks were present. Compared with traditional MMMs, SSMs has high loading of Silicalite-1 particles. Based on Figure 6, it seems that the zeolite crystals coverage is complete even when the concentration of dip-coating suspension is lower than 3 wt %, which is different with Figure 5 (incomplete coverage when zeolite concentration is <3 wt %). This might be the result of poor adhesion between zeolite crystals and Teflon substrate, which makes sample preparation difficult (long travel between lab and SEM facility).

Figure 7 shows the XRD patterns of Silicalite-1/PDMS MMMs prepared with different Silicalite-1 loadings. As illustrated in Figure 7, the pure Silicalite-1 crystal exhibits characteristic peaks at about 7.94° and 8.90°. For the MMMs, the increase of Silicalite-1 content leads to the increase in the peak intensities at about 7.94°, 8.90°, and 23.12° in comparison with the pure PDMS membrane.[37] Figure 8 shows the XRD patterns of

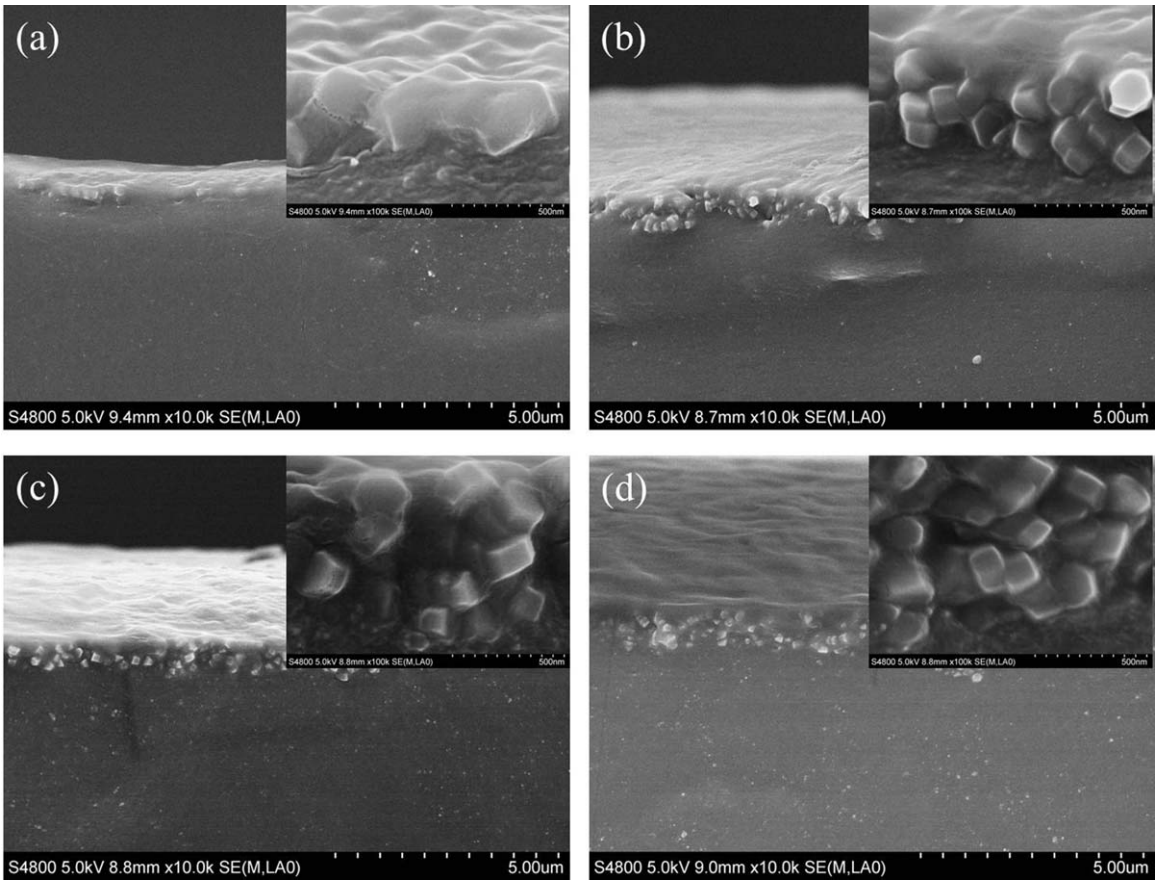

Figure 6. Cross-section morphologies of SSMs with different Silicalite-1 particles suspensions concentrations, (a) 0.4 wt %, (b) 1.0 wt %, (c) 2.0 wt %, and (d) 3.0 wt %.

Silicalite-1/PDMS SSMs prepared with Silicalite-1 particles suspensions with various concentrations. With the increase of Silicalite-1 concentrations, the intensity of Silicalite-1 peaks increase accordingly.

Figure 9 shows the thermal stability of pure PDMS membrane and Silicalite-1/PDMS MMMs prepared with different Silicalite-1 loadings. It can be seen from Figure 9 that the addition of Silicalite-1 particles improves the thermal stability of PDMS

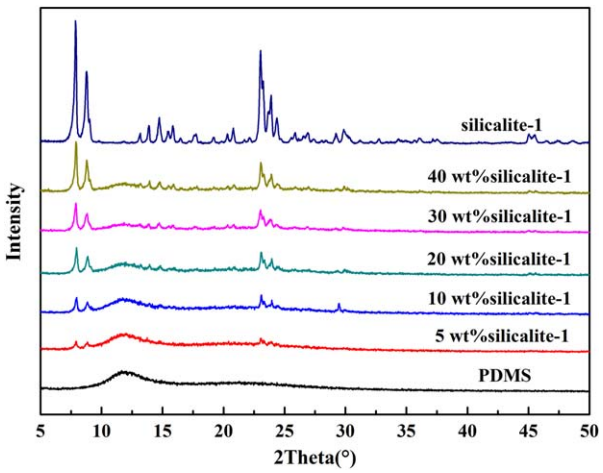

Figure 7. XRD patterns of Silicalite-1/PDMS MMMs prepared with different Silicalite-1 loadings. [Color figure can be viewed in the online issue, which is available at wileyonlinelibrary.com.]

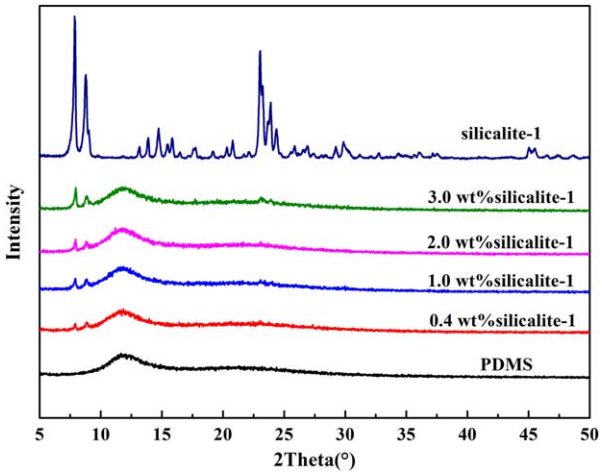

Figure 8. XRD patterns of Silicalite-1/PDMS SSMs prepared with Silicalite-1 particles suspensions with different concentrations. [Color figure can be viewed in the online issue, which is available at wileyonlinelibrary.com.]

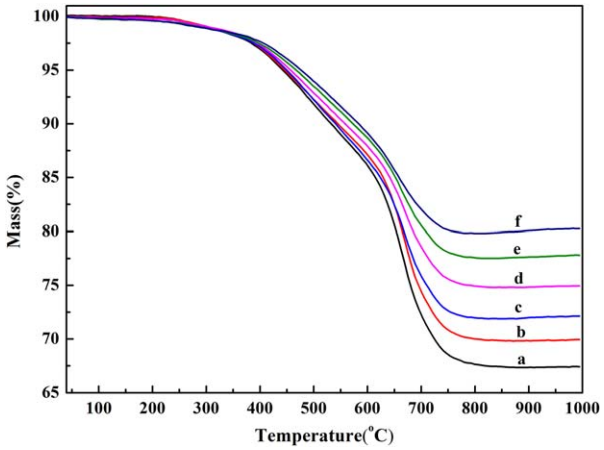

Figure 9. TGA of Silicalite-1/PDMS MMMs prepared with different Silicalite-1 loadings (a) 0 wt %, (b) 5 wt %, (c) 10 wt %, (d) 20 wt %, (e) 30 wt %, and (f) 40 wt %. [Color figure can be viewed in the online issue, which is available at wileyonlinelibrary.com.]

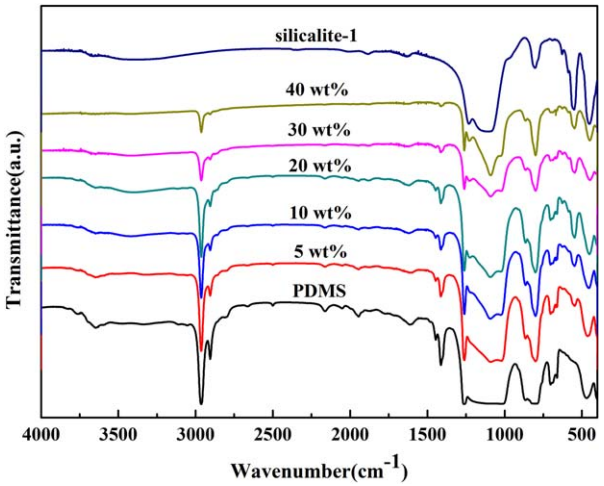

Figure 11. FT-IR of Silicalite-1/PDMS MMMs prepared with different Silicalite-1 loadings. [Color figure can be viewed in the online issue, which is available at wileyonlinelibrary.com.]

MMMs. The initial decomposition temperature[43] increased from 440°C for the pure PDMS membrane to 476°C for the 40% MMMs. The thermal stability of the MMMs increased with the Silicalite-1 loadings. The possible explanation was the presence of Silicalite-1 particles probably helps increase the adsorption of thermal energy and thus protected PDMS from thermal attack.[44,45] Figure 10 shows the thermal stability of pure PDMS membrane and Silicalite-1/PDMS SSMs prepared with different Silicalite-1 particles suspensions concentrations. Compared with the MMMs, the thermal stability of SSMs is lower. This is mainly because the concentrations of Silicalite-1 particles in MMMs are higher than those in SSMs. Combined with Figure 9 and Figure 10, the residue weight of 3 wt % SSMs is 70.22%. The residue weight of 3 wt % SSMs is between 5 and 10 wt % MMMs. This indicates that the zeolite concentration in 3 wt % SSM is lower than 10 wt % MMMs. However, SSM also has a pure PDMS layer, which suggests that zeolite concentration in the separation layer is much higher than the 10 wt % MMM. But the total Silicalite-1 particles content of 3 wt % Silicalite-1/PDMS SSMs is not high, similar to 10 wt % MMM.

Figures 11 and 12 show the FT-IR spectra of pure PDMS membrane, MMMs, and SSMs. As exhibited in Figure 11, the adsorption peaks at 3440 and 1110 cm^{-1} correspond to stretching and asymmetric stretching vibrations of Si-OH on the Silicalite-1 particles surface, respectively. The peaks at 803 and 467 cm^{-1} represent the asymmetric stretching and bending vibration of siloxane groups (Si-O-Si), respectively. A weak band at 2960 cm^{-1} is ascribed to symmetric vibration of the hydrophobic C–H groups in the FT-IR spectrum of PDMS membrane.[12] As shown in Figures 11 and 12, all MMMs and SSMs have similar IR spectra between 400 and 4000 cm^{-1}. Compare the spectrums of pure PDMS membrane with that of the MMMs and SSMs, no new absorption peak could be

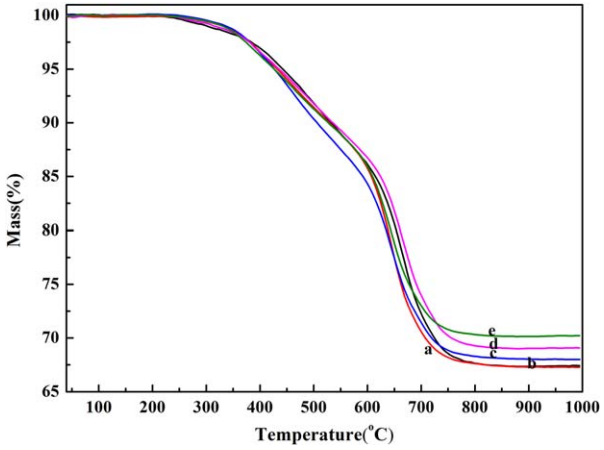

Figure 10. TGA of Silicalite-1/PDMS SSMs prepared with different Silicalite-1 particles suspensions concentrations (a) 0 wt %, (b) 0.4 wt %, (c) 1.0 wt %, (d) 2.0 wt %, and (e) 3.0 wt %. [Color figure can be viewed in the online issue, which is available at wileyonlinelibrary.com.]

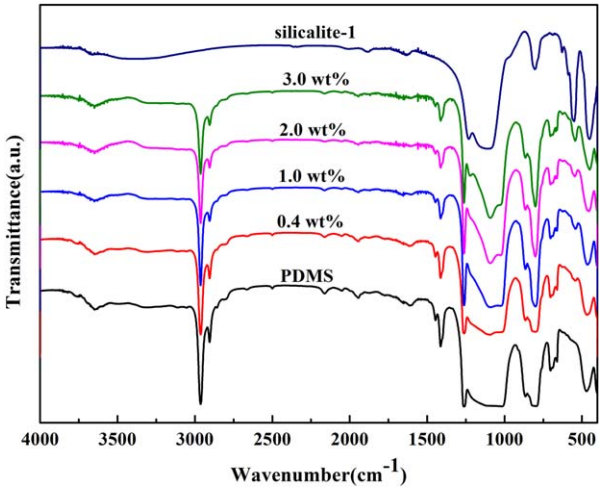

Figure 12. Silicalite-1/PDMS SSMs prepared with different Silicalite-1 particles suspensions concentrations. [Color figure can be viewed in the online issue, which is available at wileyonlinelibrary.com.]

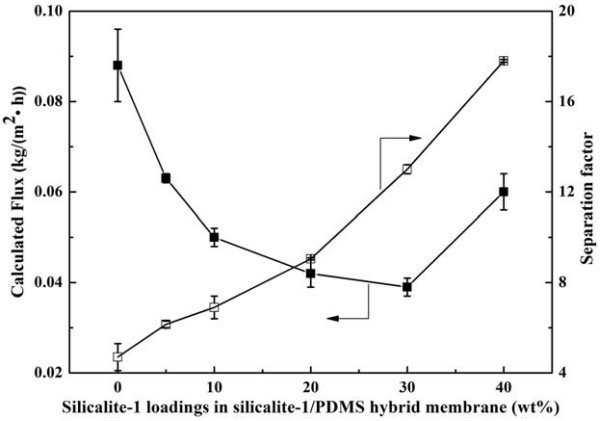

Figure 13. Performance of Silicalite-1/PDMS MMMs for pervaporation separation of ethanol–water mixtures with different Silicalite-1 loadings.

observed, which demonstrates that Silicalite-1 particles is only physically dispersed in the MMMs and SSMs.

Pervaporation Performance of MMMs and SSMs

Effect of Silicalite-1 Particles Content. The effect of Silicalite-1 loadings on the performance of Silicalite-1/PDMS MMMs for pervaporation separation of ethanol–water mixtures is shown in Figure 13. In all pervaporation separation experiments, a 5.0 wt % ethanol solution (in water) was used as feed. The fluxes were normalized to thickness of 100 μm. Pure PDMS membrane had separation factor of 4.8 and flux of 0.091 kg.m^{-2}.h^{-1}. As shown in Figure 13, the permeation flux of the membrane as a function of the Silicalite-1 loadings is found to reach a minimum at 10 wt %, whereas the separation factor increases as Silicalite-1 loadings increases. With the continued increase of the Silicalite-1 loadings, there is little change in permeation flux. The increase of ethanol–water separation factor can be attributed to the presence of hydrophobic Silicalite-1 crystals, which enhances the preferential adsorption of hydrophobic ethanol over the hydrophilic water. With the increase of Silicalite-1 particles content from 0 to 40 wt %, the separation factor increased from 4.8 to 17.9. These can be explained by the enhanced physical cross-linking and the restricted plasticization as more Silicalite-1 particles are introduced.[27,29] Silicalite-1 particles can yield more polymer–particle interfacial area, which could effectively restrict the membrane swelling and plasticization and improve the membrane separation performance.[36]

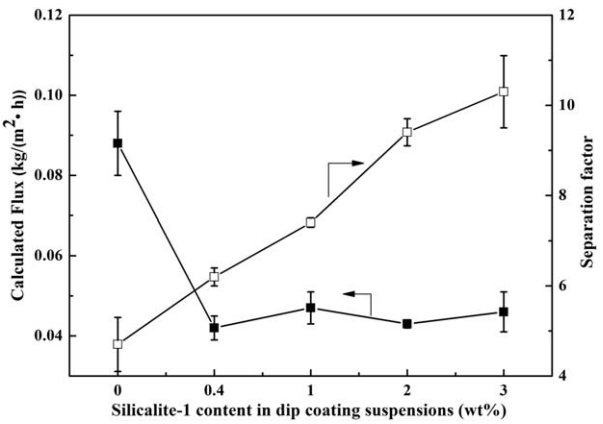

Figure 14. Performance of Silicalite-1/PDMS SSMs for pervaporation separation of ethanol–water mixtures with different Silicalite-1 particles suspensions concentrations.

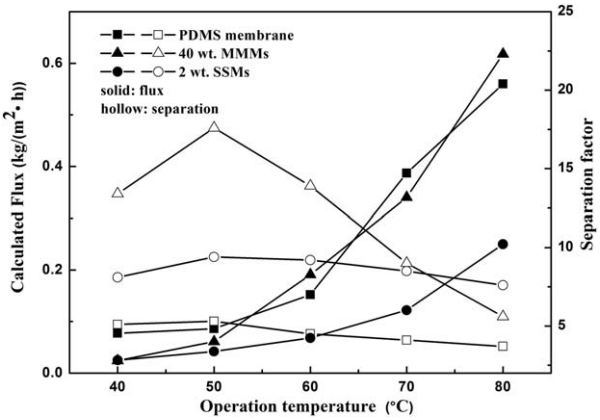

Figure 15. Effect of feed temperature on pervaporation performance of the pure membrane, MMMs, and SSMs at the ethanol concentration of 5 wt %.

Figure 14 shows the performance of SSMs with different Silicalite-1 particles suspensions concentrations. As the Silicalite-1 particles suspensions concentrations increased, the separation factor increased. This trend is similar to MMMs. When the suspensions concentrations of Silicalite-1 particles reached 3 wt %, the separation factor was 10.4, which was ~217% increase over pure PDMS membrane. This is the result of more selective permeation through Silicalite-1 particles crystals.

Comparing Figures 13 and 14, we found that the separation factor of 10 wt % Silicalite-1/PDMS MMMs and 3 wt % Silicalite-1/PDMS SSMs are 6.8 and 10.4, respectively. The total Silicalite-1 particles content of 10 wt % Silicalite-1/PDMS MMMs is more than that of 3 wt % Silicalite-1/PDMS SSMs; however, the separation factor is only 65% of SSMs.

Effect of Feed Temperature. Temperature is a critical operation parameter that affects pervaporation performance substantially. Figure 15 shows the effect of feed temperature on pervaporation performance of the pure membrane, MMMs and SSMs with 5 wt % ethanol/water as feed. Generally, with the increase of operating temperature, total flux increases and separation factor decreases. But in this work, MMMs and SSMs appear that as the feed temperature increases, the total flux increase and the separation factor increased to a maximum and then decreased at 50°C. The reason is that Silicalite-1 particles in the membranes made membrane structure changed which makes the absorption and diffusion of ethanol molecules easier than that of the water molecules. But when temperature increased from 50 to 80°C, the slight increase of ethanol solubility selectivity and the sharp decrease of ethanol diffusion selectivity caused the decrease of the separation factor.[12] When the temperature increased to 50°C, the separation factor of 40 wt % MMMs and 2 wt % SSMs are 17.9 and 9.4, respectively. From 50 to 80°C, the separation factor of SSM decreased slightly ~18% and MMM exhibited ~69% drop. When the operating temperature

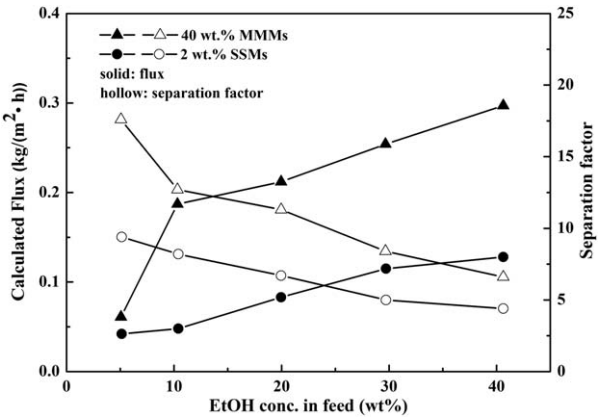

Figure 16. Effect of ethanol concentration on pervaporation performance of MMMs and SSMs.

increases, both the vapor pressure difference (activity or driving force) across the membrane and the free volume of MMMs and SSMs increase.[46] Both are positive for diffusion because that makes the polymer chains more flexible. From Figure 16, we can also see that when the temperature increased from 40 to 80°C, the selectivity of SSMs decrease a similar proportion compared with the PDMS membrane. However, the separation factor of 2 wt % SSMs is higher than that of 40 wt % MMMs at 80°C. As the increase of temperatures, the adhesion between Silicalite-1 particles and PDMS could fall. Therefore, the selective of MMMs decreased obviously. The increase of temperature leads to an increase in the driving force although the vapor pressure at the permeate side is unaffected. Therefore, the increasing diffusion of both permeating molecules gives a higher flux, whereas the selectivity decreased.[36] Because the SSM has a thick layer of PDMS, the thermal stability of SSM is similar to PDMS membrane.

Effect of Feed Composition. Feed composition has an important effect on the solubility and diffusion coefficient of preferentially sorbed component in the membrane.[47] The effect of ethanol feed content on separation factors and total fluxes of MMMs and SSMs at 50°C are depicted in Figure 16. It can be seen that separation factor decreases and permeation flux increases with increasing ethanol concentration. In a binary feed mixture, if the polarity difference between the membrane material and the target component is lower than the other component, the membrane will be more swelled by target component and shows preferential selectivity to the target component, to some extent. The polarity of ethanol was more similar to that of cross-linked PDMS than water. By increasing the ethanol concentration, ethanol in the feed phase had more sorption interaction with PDMS membrane phase and the sorption of the ethanol made the PDMS layer more swollen. Thus, segments of the PDMS polymer had more freedom of volume and mobility. By increasing the polymer chain mobility, thermal motion of these segments enhanced the diffusion rate of both permeating components.[48] Therefore, the total permeation fluxes increased as the ethanol concentration increased.

Resistance Model for Gas Transport in SSMs. The ethanol and water flow though the SSMs as described in Figure 17 can also be analyzed using the resistance model. It is assumed that the ethanol and water flow is strictly vertical to the surface of the membrane. No mixing is assumed between these two pathways.[49] The overall resistance for ethanol is:

$$R_{\mathrm{EtOH}}=\frac{[(R_2)_{\mathrm{EtOH}}+(R_2)'_{\mathrm{EtOH}}]\times[(R_1)_{\mathrm{EtOH}}+(R_1)'_{\mathrm{EtOH}}]}{[(R_2)_{\mathrm{EtOH}}+(R_2)'_{\mathrm{EtOH}}]+[(R_1)_{\mathrm{EtOH}}+(R_1)'_{\mathrm{EtOH}}]} \quad (3)$$

For water:

$$R_{\mathrm{H_2O}}=\frac{[(R_2)_{\mathrm{H_2O}}+(R_2)'_{\mathrm{H_2O}}]\times[(R_1)_{\mathrm{H_2O}}+(R_1)'_{\mathrm{H_2O}}]}{[(R_2)_{\mathrm{H_2O}}+(R_2)'_{\mathrm{H_2O}}]+[(R_1)_{\mathrm{H_2O}}+(R_1)'_{\mathrm{H_2O}}]} \quad (4)$$

In the formula (3) and (4),

$$[(R_2)_{\mathrm{EtOH}}+(R_2)'_{\mathrm{EtOH}}]=\frac{rl}{m(J_{\mathrm{Silicalite-1}})_{\mathrm{EtOH}}}+\frac{rL}{m(J_{\mathrm{PDMS}})_{\mathrm{EtOH}}} \quad (5)$$

$$[(R_1)_{\mathrm{EtOH}}+(R_1)'_{\mathrm{EtOH}}]=\frac{r(l+L)}{(1-m)(J_{\mathrm{PDMS}})_{\mathrm{EtOH}}} \quad (6)$$

$$[(R_2)_{\mathrm{H_2O}}+(R_2)'_{\mathrm{H_2O}}]=\frac{rl(\alpha_{\mathrm{Silicalite-1}})_{\mathrm{EtOH/H_2O}}}{m(J_{\mathrm{Silicalite-1}})_{\mathrm{EtOH}}}+\frac{rL(\alpha_{\mathrm{PDMS}})_{\mathrm{EtOH/H_2O}}}{m(J_{\mathrm{PDMS}})_{\mathrm{EtOH}}} \quad (7)$$

$$[(R_1)_{\mathrm{H_2O}}+(R_1)'_{\mathrm{H_2O}}]=\frac{r(l+L)(\alpha_{\mathrm{PDMS}})_{\mathrm{EtOH/H_2O}}}{(1-m)(J_{\mathrm{PDMS}})_{\mathrm{EtOH}}} \quad (8)$$

where r is the resistance of Silicalite-1 membrane (1 m × 1 m × 1 μm), m is the coverage of Silicalite-1 particles in SSMs, J is the flux, and α is the separation factor.

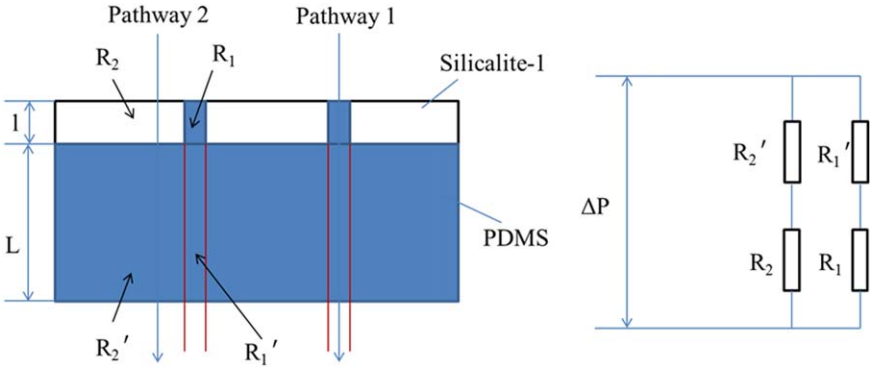

Figure 17. The resistance model of SSMs. [Color figure can be viewed in the online issue, which is available at wileyonlinelibrary.com.]

The separation factor of SSMs is:

$$(\alpha_{SSMs})_{\frac{EtOH}{H_2O}} = \frac{R_{H_2O}}{R_{EtOH}} = \frac{\left[\frac{l(\alpha_{Silicalite-1})_{EtOH/H_2O}}{m(J_{Silicalite-1})_{EtOH}} + \frac{L(\alpha_{PDMS})_{EtOH/H_2O}}{m(J_{PDMS})_{EtOH}}\right] \times \left[\frac{(l+L)(\alpha_{PDMS})_{EtOH/H_2O}}{(1-m)(J_{PDMS})_{EtOH}}\right]}{\left[\frac{l(\alpha_{Silicalite-1})_{EtOH/H_2O}}{m(J_{Silicalite-1})_{EtOH}} + \frac{L(\alpha_{PDMS})_{EtOH/H_2O}}{m(J_{PDMS})_{EtOH}}\right] + \left[\frac{(l+L)(\alpha_{PDMS})_{EtOH/H_2O}}{(1-m)(J_{PDMS})_{EtOH}}\right]} = \frac{\left[\frac{l}{m(J_{Silicalite-1})_{EtOH}} + \frac{L}{m(J_{PDMS})_{EtOH}}\right] \times \left[\frac{(l+L)}{(1-m)(J_{PDMS})_{EtOH}}\right]}{\left[\frac{l}{m(J_{Silicalite-1})_{EtOH}} + \frac{L}{m(J_{PDMS})_{EtOH}}\right] + \left[\frac{(l+L)}{(1-m)(J_{PDMS})_{EtOH}}\right]} \quad (9)$$

From the above comparison, it is obvious that *m* and *l*/L has big impact on the separation factor of SSMs. The increase of the *m* and *l*/L may improve the separation factor of SSMs.

CONCLUSIONS

Surface sieving membranes (SSMs) were successfully prepared by using Silicalite-1 particles and PDMS. SEM graphs showed that the adhesion of SSMs between the polymer phase and Silicalite-1 particles was good because no voids and cracks were present. The membranes containing Silicalite-1 showed high selectivity. In the case of the same Silicalite-1 particles content, the selectivity of SSMs is higher than that of MMMs. Ten percentage of Silicalite-1/PDMS MMMs contain more Silicalite-1 particles than 3% Silicalite-1/PDMS SSMs, but the separation factor is lower than that of SSMs. The separation factor of 10% Silicalite-1/PDMS MMMs and 3% Silicalite-1/PDMS SSMs are 6.8 and 10.4, respectively. When the temperature increased from 40 to 80°C, the selectivity of 2 wt % SSMs changed slightly but the selectivity of 40 wt % MMMs decreased from 17.9 to 5.6 when the temperature ranged from 40 to 80°C. When the temperature reached 80°C, the separation factor of 2 wt % SSMs is higher than that of 40 wt % MMMs.

ACKNOWLEDGMENTS

The authors acknowledge the financial supports from National 863 Project (No: 2012AA050104) and Advanced Coal Processing Project of Chinese Academic Sciences (No: XDA07040401).

REFERENCES

1. Dubey, V.; Pandey, L. K.; Saxena, C. *J. Membr. Sci.* **2005**, *251*, 131.
2. Liang, B.; Pan, K.; Li, L.; Giannelis, E. P.; Cao, B. *Desalination* **2014**, *347*, 199.
3. Han, Y. J.; Wang, K. H.; Lai, J. Y.; Liu, Y. L. *J. Membr. Sci.* **2014**, *463*, 17.
4. Bowen, T. C.; Noble, R. D.; Falconer, J. L. *J. Membr. Sci.* **2004**, *245*, 1.
5. Sebastian, V.; Mallada, R.; Coronas, J.; Julbe, A.; Terpstra, R. A.; Dirrix, R. W. *J. Membr. Sci.* **2010**, *355*, 28.
6. Zhou, K.; Zhang, Q. G.; Han, G. L.; Zhu, A. M.; Liu, Q. L. *J. Membr. Sci.* **2013**, *448*, 93.
7. Ong, Y. K.; Wang, H.; Chung, T. S. *Chem. Eng. Sci.* **2012**, *79*, 41.
8. Jiang, X.; Gu, J.; Shen, Y.; Wang, S.; Tian, X. *Desalination* **2011**, *265*, 74.
9. Fu, Y. J.; Lai, C. L.; Chen, J. T.; Liu, C. T.; Huang, S. H.; Hung, W. S.; Lee, K. R. *Chem. Eng. Sci.* **2014**, *111*, 203.
10. Jadav, G. L.; Aswal, V. K.; Bhatt, H.; Chaudhari, J. C.; Singh, P. S. *J. Membr. Sci.* **2012**, *415*, 624.
11. Zhan, X.; Li, J.; Huang, J.; Chen, C. *Appl. Biochem. Biotechnol.* **2010**, *160*, 632.
12. Sun, D.; Li, B. B.; Xu, Z. L. *Desalination* **2013**, *322*, 159.
13. Martínez, R.; Teresa Sanz, M.; Beltrán, S. *J. Membr. Sci.* **2013**, *428*, 371.
14. Li, S. Y.; Srivastava, R.; Parnas, R. S. *J. Membr. Sci.* **2010**, *363*, 287.
15. Zhan, X.; Li, J.; Fan, C.; Han, X. *Chin. J. Polym. Sci.* **2010**, *28*, 625.
16. Peng, F.; Pan, F.; Li, D.; Jiang, Z. *Chem. Eng. J.* **2005**, *114*, 123.
17. Qi, R.; Wang, Y.; Li, J.; Zhao, C.; Zhu, S. *J. Membr. Sci.* **2006**, *280*, 545.
18. Liu, W.; Ji, S. L.; Guo, H. X.; Gao, J.; Qin, Z. P. *J. Appl. Polym. Sci.* **2014**, 131.
19. Niemistö, J.; Kujawski, W.; Keiski, R. L. *J. Membr. Sci.* **2013**, *434*, 55.
20. Kulprathipanja, S.; Li, N. N.; Neuzil, R. W. U.S. Patent 4,740,219, April 26, **1988**.
21. Kulprathipanja, S.; Li, N. N.; Neuzil, R. W. U.S. Patent 5,127,925, July 7, **1992**.
22. Chung, T. S.; Jiang, L. Y.; Li, Y.; Kulprathipanja, S. *Prog. Polym. Sci.* **2007**, *32*, 483.
23. Cong, H.; Radosz, M.; Towler, B. F.; Shen, Y. *Sep. Purif. Technol.* **2007**, *55*, 281.
24. Goh, P. S.; Ismail, A. F.; Sanip, S. M.; Ng, B. C.; Aziz, M. *Sep. Purif. Technol.* **2011**, *81*, 243.
25. Peng, F.; Jiang, Z.; Hu, C.; Wang, Y.; Xu, H.; Liu, J. *Sep. Purif. Technol.* **2006**, *48*, 229.
26. Shirazi, Y.; Ghadimi, A.; Mohammadi, T. *J. Appl. Polym. Sci.* **2012**, *124*, 2871.
27. Liu, G.; Xiangli, F.; Wei, W.; Liu, S.; Jin, W. *Chem. Eng. J.* **2011**, *174*, 495.
28. Andersson, C.; Hedlund, J. *J. Membr. Sci.* **2008**, *313*, 120.
29. Yi, S.; Su, Y.; Wan, Y. *J. Membr. Sci.* **2010**, *360*, 341.
30. Chen, H.; Li, Y.; Yang, W. *J. Membr. Sci.* **2007**, *296*, 122.
31. Keasler, S. J.; Bai, P.; Tsapatsis, M.; Siepmann, J. I. *Fluid Phase Equilib.* **2014**, *362*, 118.
32. Zhang, X.; Zhu, M.; Zhou, R.; Chen, X.; Kita, H. *Sep. Purif. Technol.* **2011**, *81*, 480.
33. Zhou, H.; Su, Y.; Chen, X.; Wan, Y. *Sep. Purif. Technol.* **2011**, *79*, 375.
34. Zheng, D.; Liu, X.; Hu, D.; Li, M.; Zhang, J.; Zeng, G.; Sun, Y. *RSC Adv.* **2014**, *4*, 10140.
35. Motuzas, J.; Julbe, A.; Noble, R. D.; Van Der Lee, A.; Beresnevicius, Z. *J. Microporous Mesopor. Mater.* **2006**, *92*, 259.

36. Wang, L.; Han, X.; Li, J.; Zhan, X.; Chen, *J. Chem. Eng. J.* **2011**, *171*, 1035.
37. Li, B.; Xu, D.; Jiang, Z. Y. *J. Membr. Sci.* **2008**, *322*, 293.
38. Tröber, O. T.; Richter, H. R.; Weyd, M. W.; Brueschke, E. T. H. B.; Tusel, G. T. *Proced. Eng.* **2012**, *44*, 1587.
39. Bowen, T. C.; Meier, R. G.; Vane, L. M. *J. Membr. Sci.* **2007**, *298*, 117.
40. Choi, S. Y.; Lee, Y. J.; Park, Y. S.; Ha, K.; Yoon, K. B. *J. Am. Chem. Soc.* **2000**, *122*, 5201.
41. Yoon, K. B. *Bull. Korean Chem. Soc.* **2006**, *27*, 17.
42. Zhang, B.; Zhou, M.; Liu, X. *Adv. Mater.* **2008**, *20*, 2183.
43. Adnadjevic, B.; Jovanovic, J. *J. Appl. Polym. Sci.* **2000**, *77*, 1171.
44. Kim, H.; Kim, H. G.; Kim, S.; Kim, S. S. *J. Membr. Sci.* **2009**, *344*, 211.
45. Sun, Y.; Zhang, Z.; Wong, C. P. *J. Colloid Interface Sci.* **2005**, *292*, 436.
46. Peng, M.; Vane, L. M.; Liu, S. X. *J. Hazard. Mater.* **2003**, *98*, 69.
47. Feng, X.; Huang, R. Y. *Ind. Eng. Chem. Res.* **1997**, *36*, 1048.
48. Xiangli, F.; Chen, Y.; Jin, W.; Xu, N. *Ind. Eng. Chem. Res.* **2007**, *46*, 2224.
49. Li, K. Ceramic Membranes for Separation and Reaction; John Wiley & Sons, **2007**, 117.